Oscillatory Excitation Transfer in Dithiaanthracenophane: Quantum Beat in a Coherent Photochemical Process in Solution†

Iwao Yamazaki,*,‡ Seiji Akimoto,‡ Tomoko Yamazaki,‡ Shin-ichiro Sato,‡ and Yoshiteru Sakata§

Department of Molecular Chemistry, Graduate School of Engineering, Hokkaido University, Sapporo 060-8628, Japan, and The Institute of Scientific and Industrial Research, Osaka University, Mihoga-oka, Ibaraki, Osaka 567-0047, Japan

Received: June 27, 2001; In Final Form: November 28, 2001

The intramolecular electronic excitation transfer in dithiaanthracenophane (DTA) in THF solution has been investigated by probing the fluorescence anisotropy decay with a femtosecond up-conversion method. In DTA, two anthracene rings are known to be stacked parallel, but with nearly orthogonal orientation. There appeared a damped oscillation of an apparent period of 1.2 ± 0.2 ps and a damping time constant of 1.0 ± 0.1 ps. It has been found that the oscillatory behavior is consistent with the recurrence motion of an excitation between two anthracene moieties, from a theoretical analysis following a manner of Wynne and Hochstrasser (Wynne, K.; Hochstrasser, R. M. *J. Raman Spectrosc.* **1995**, *26*, 561). The magnitude of the dipole−dipole energy transfer interaction is estimated to be 40 cm^{-1} which is in an acceptable agreement with the experimental value (29 cm^{-1}) deduced from the oscillation period. In comparison with the similar case of 2,2′-binaphthyl (BN) reported by Zhu et al. (Zhu, F.; Galli, C.; Hochstrasser, R. M. *J. Chem. Phys*. **1993**, *98*, 1042), the electronic dephasing time T_2' is significantly longer in DTA (1.0 ps) than in BN (0.2 ps). The longer dephasing time in DTA can be explained as arising from a much more fixed and rigid dimeric conformation than in BN.

1. Introduction

Since the Förster mechanism[1] of intermolecular excitation energy transfer due to a dipole−dipole interaction was formulated, many works have been reported for molecules in fluid solution, polymer films, and solid matrixes. The energy transfer dynamics has been discussed in terms of the very-weak coupling limit in the Förster theory, the interaction energy $\beta < 1$ cm^{-1}, and the irreversible energy transfer rate $w < 10^{11}$ s^{-1}. On the other hand, recent investigations have focused on the intramolecular energy transfer in organized molecular systems in which reacting molecules of donor and acceptor are connected chemically with close proximity and specific orientation. Molecules in such systems can be coupled with much stronger interaction ($\beta \approx 10-50$ cm^{-1}) and therefore they may undergo ultrafast energy transfer reaction ($w \approx 10^{12}-10^{13}$ s^{-1}). According to the Förster theory,[1] the energy transfer dynamics under such condition can be expressed in terms of the *intermediate coupling case*.

With bichromophoric molecules, for example, in which two identical chromophores are connected through a weakly conjugating linkage, the interchromophore energy transfer occurs via recurrence motion of excitation between the two chromophores. By photoexciting coherently the "exciton" states, i.e., the superposition states of two locally excited states, which are split by an interaction energy 2β, the excitation moves back and forth between the coupled chromophores. To observe such a recurrence experimentally, (1) the spectral coherence of excitation light pulse must be broad enough to span the two eigenstates so that the off-diagonal density matrix elements may become populated and therefore select localized states, (2) the period of the coherence oscillation should be shorter than the electronic dephasing time, and (3) the lab frame orientation of the electronic transition moments of absorption or emission is different between the different halves of bichromophore system. In the case under these conditions (1)−(3), the recurrence may appear as a damped oscillation on the fluorescence anisotropy decay which is defined as the difference of the probe signals parallel ($I_{||}$) and perpendicular ($I_{\perp}$) to the polarization plane of the excitation laser, i.e., $r(t) = \{I_{||}(t) - I_{\perp}(t)\}/\{I_{||}(t) + 2I_{\perp}(t)\}$.

Whether or not such a predicted macroscopic quantum coherence will be observable depends on the strength of the coupling of the exciton to the heat bath. In fact, the quantum mechanical treatments including explicitly the dephasing paths predicted a noticeable effect of the initial electronic coherence on the fluorescence anisotropy associated with the energy transfer in a pair of chromophores. Rahman et al.[2] and Knox and Gülen[3] pointed out that the stochastic Liouville equation using the density matrix gives an anisotropy larger than 0.4, i.e., the initial anisotropy observed in a collection of randomly oriented single molecules. Matro and Cina[4] calculated the time course of the fluorescence anisotropy based on the Redfield theory, and demonstrated an important role of vibronic transitions. Therefore, one can expect to observe the electronic coherence or the recurrence of energy transfer by using molecular systems of an appropriate arrangement of chromophores.

Hochstrasser and co-workers[5,6] studied the coherent excitation energy transfer between two identical chromophores in 9,9′-bifluorene and 2,2′-binaphthyl in different solvents at room temperature; the anisotropy decay of transient absorption in binaphthyl exhibited a damped oscillation corresponding to the

† Part of the special issue "Noboru Mataga Festschrift".

* Author to whom correspondence should be addressed. Phone: 81-11-706-6606. Fax: 81-11-709-2037. E-mail: yamiw@eng.hokudai.ac.jp.

‡ Hokkaido University.

§ Osaka University.

10.1021/jp012455w CCC: $22.00
Published on Web 02/16/2002

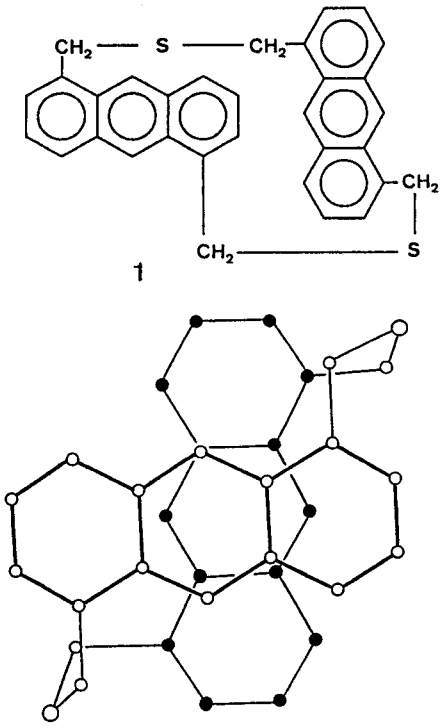

Figure 1. (a) Molecular formula of dithiaanthracenophane (DTA), and (b) a view of DTA on least-squares plane defined with an anthracene ring determined from X-ray analysis.

excitation recurrence associated with the interaction energy (2β) of 41 cm^{-1} and the dephasing time (T_2') of 0.2 ps. Although their experimental data of damped oscillation are quite impressive as evidenced by the close agreement with the theoretical prediction, the contribution of the oscillating part is very small relative to the overall anisotropy signal. This may be accounted for as due to a broad conformational distribution of the dimeric structure of binaphthyl in solution which makes the macroscopic energy transfer dynamics incoherent. To observe the coherent dynamics more precisely, it is necessary to use a molecular system in which two chromophores are connected rigidly so that the dimeric conformation is fixed with a specific energy transfer interaction and a well-defined energy level structure.

We have studied the intramolecular excitation transfer in dithia(1,5)[3,3]-anthracenophane (DTA)[7] having a pair of identical chromophores stacked rigidly. The molecular structure determined from X-ray crystallography is shown in Figure 1. Two anthracene rings are connected through two thioethers at α positions almost parallel (dihedral angle, 5.0°) with an interplanar distance of 3.41 Å and one of the rings is rotated by 88.5° around the center of the anthracene ring.[7] The spatial arrangement of the two chromophores in DTA is suitable for examining the coherent dynamics of excitation transfer with a rigid and confined conformation of the dimeric structure. The nearly orthogonal orientation of the two anthracene rings, and their respective transition dipole moment vectors, is expected to enable selective detection of the emission from each chromophore. The fluorescence up-conversion method was adapted for measurement of fluorescence anisotropy decays of DTA in THF solution at room temperature. A damping oscillation appeared on the anisotropy decay in the femtosecond time region. We analyzed the anisotropy oscillation following the theoretical framework for the coherent energy transfer formulated by Wynne and Hochstrasser.[8−10] Finally, the results are compared with the case of 2,2′-binaphthyl reported by Hochstrasser and co-workers.[6]

2. Experimental

Reaction of 1,5-di(methoxycarbonyl)anthracene[11] with $LiAlH_4$ in THF, followed by bromination with PBr_3 in benzene gave 1,5-di(bromomethyl) anthracene in 20% yield. A coupling reaction with Na_2S was carried out in a mixed solvent of benzene, ethanol, and H_2O (44:9:1). After workup and column chromatography (silica gel, benzene−hexane), DTA was obtained in 33% yield along with an oligomer. The other possible isomer with eclipsed orientation was not found in the reaction mixture.

The excitation source was the second harmonics of a Ti:Sapphire laser (Spectra Physics Tsunami, 816 nm, 80 MHz) pumped with a diode-pumped solid state laser (Spectra Physics, Millenia X). The output laser pulse had a pulse width of 80 fs (fwhm), and an average energy 16 nJ at 816 nm. Approximately half of the laser beam was frequency doubled in a BBO crystal for the sample excitation (0.5 nJ at 408 nm), and the remainder was used for the gating pulse. The gating pulse passed through a variable delay line using a translation stage (Sigma STM-20X) with 1.0 μm per step (corresponding to the delay time of 6.7 fs) under computer control. The fluorescence emission and the gating pulse were focused into a 0.5 mm BBO crystal by a 5.0 cm focal length lens. The wavelength of up-conversion signal was adjusted by rotating the BBO crystal in a type 1 phase matching geometry. The wavelength of the detected signal, in practice, was approximately 290 nm, corresponding to a fluorescence wavelength of 450 nm. The sum frequency signal was both filtered and frequency selected using a monochromator (JASCO CT-10) and a single-photon counting apparatus equipped with a Hamamatsu R106UH photomultiplier.

The spectral width of the excitation laser pulse (the uncertainty-principle limited pulse) is estimated from the relation $\Delta\nu\cdot\Delta t = 0.44$ between the spectral width $\Delta\nu$ and the laser pulse width Δt. From the pulse width of the laser used in this study, $\Delta t =$ 80 fs, the spectal width is $\Delta\nu$ (fwhm) = 190 cm^{-1}. Since the magnitude of energy transfer interaction 2β for DTA is calculated to be 40 cm^{-1} as shown in Section 4.3, the two eigenstates split by 2β may be excited coherently by using the present light source.

For the time-dependent fluorescence anisotropy, the polarization components of upconversion signals, i.e., parallel ($I_{||}$) and perpendicular ($I_{\perp}$) to the polarization plane of the excitation laser light, were measured alternately. The data taken several times from alternate measurements were collected, and the anisotropy $r(t) = \{I_{||}(t) - I_{\perp}(t)\}/\{I_{||}(t) + 2I_{\perp}(t)\}$ were calculated.

All experiments were carried out at room temperature. The sample DTA was dissolved in THF with concentration of 10^{-5} M, and the sample cell of 1-mm thick was used.

3. Results

3.1. Absorption and Fluorescence Spectra. Figure 2 shows absorption and fluorescence spectra of DTA in THF. The absorption spectrum of DTA is similar to the anthracene spectrum with several vibrational bands. The stationary fluorescence spectrum in THF exhibits only a diffuse and broad band centered at 469 nm (curve 2 in Figure 2), which is different obviously from the mirror image of the absorption band profile. Previously, we examined the picosecond time-resolved fluorescence spectra (see Figure 2 of ref 7) in relation to the excimer formation of DTA.[7] The fluorescence spectrum in a short time region (0−25 ps) exhibits a well-defined, structured spectrum (curve 1 in Figure 2) with a mirror image of the absorption, while after 50 ps it changes into a broad and diffuse one centered at 469 nm which is identical to the stationary fluorescence

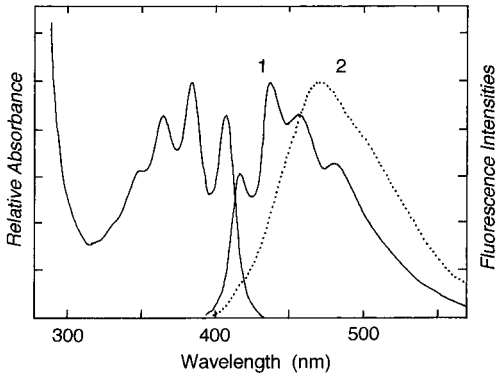

Figure 2. Absorption (left) and fluorescence (right) spectra of DTA in THF. Curve 1 is the time-resolved fluorescence spectrum in 0−25 ps, and curve 2 is the stationary fluorescence spectrum.

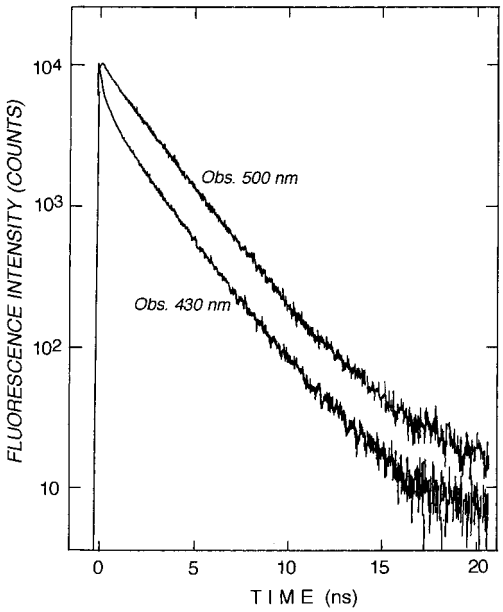

Figure 3. Fluorescence decay curves of DTA in THF, obtained with the picosecond TCPC apparatus. The wavelength of excitation is 310 nm, and the monitoring wavelengths are 430 and 500 nm.

spectrum (curve 2 in Figure 2). From analyses of the fluorescence rise and decay curves as well as the time-resolved spectra, we assigned the structured band (0∼25 ps) to a monomer fluorescence and the broad red-shifted band (after 50 ps) to an excimer fluorescence. Since we are concerned here with the time region shorter than 5 ps, then we are able to confine our discussion to the excited-state dynamics of monomeric anthracene far before the excimer formation process, but under the energy transfer interaction with another half of the bichromophore system.

3.2. Fluorescence Decays and Anisotropy Decays. Figure 3 shows the picosecond fluorescence decay curves measured with a time-correlated, single-photon counting (TCPC) apparatus. The decay curve depends on the monitoring wavelength; the decay at 430 nm is biexponential with the lifetimes of τ_F = 63 ps and 3.2 ns, while at 500 nm it is almost single exponential with τ_F = 3.2 ns. Note that the time-resolved fluorescence spectra of DTA, as mentioned above, show the spectrum of anthracene monomer in a time region of 0−25 ps. Then it follows that the 63-ps lifetime corresponds to the time constant of the excimer formation between the excited and unexcited chromophores, and that of 3.2 ns corresponds to the deactivation of the excimer state to the ground state of monomer.

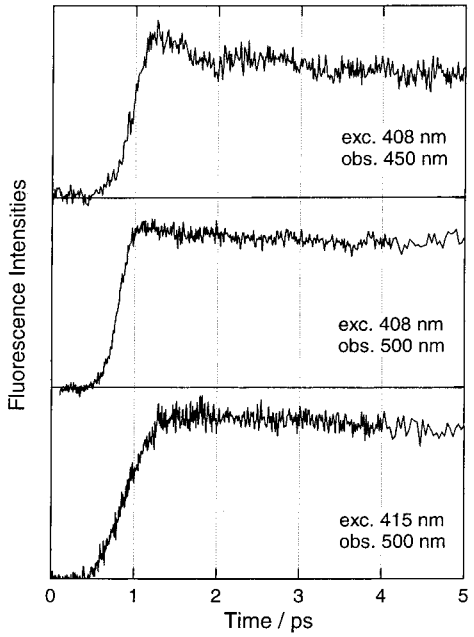

Figure 4. Femtosecond fluorescence decay curves of DTA in THF, measured with the fluorescence up-conversion apparatus for the polarization component parallel to the pump laser polarization for different wavelengths of excitation and observation.

TABLE 1: Time Constants of Picosecond Fluorescence Decay and Anisotropy Decay and the Relaxation Rates in DTA

picosecond fluorescence and anisotropy decays		
fluorescence decay (430 nm)	63 ± 1 ps	excited-state deactivation of singly excited state T_1
fluorescence decay (500 nm)	3.2 ± 0.5 ns	deactivation of an excimer
anisotropy decay	30.0 ± 1 ps	rotational diffusion
femtosecond anisotropy decay		
time period of the oscillation	1.2 ± 0.2 ps	time period $2\pi/\omega$
damping constant of the oscillation	1.0 ± 0.1 ps	dephasing time T_2'

Femtosecond fluorescence decays of DTA in THF solution at 296 K are shown in Figure 4, which were obtained by detecting the polarized fluorescence component parallel to the polarization plane of the excitation laser light. In this measurement, DTA was excited around the 0−0 band of ^1L_a absorption transition with a laser pulse (pulse width 70 fs, spectral width $\Delta\nu$ = 211 cm^{-1}) of center wavelengths of 408 nm (Figures 4a and 4b) and 415 nm (Figure 4c). When the excitation is performed at the center of 0−0 band (408 nm) and the fluorescence is monitored at 450 nm, the fluorescence decay exhibits an oscillatory pattern in the initial time region of <4 ps (Figure 4a). Monitoring the fluorescence at 500 nm, however, gives only a weak oscillation on the decay curve (Figure 4b). In an excitation at a longer wavelength band edge of the 0−0 band at 415 nm (Figure 4c), there is no oscillatory pattern, and the decay curve can be fitted with a single-exponential decay. The parameters of decay kinetics are summarized in Table 1.

Figure 5a shows the fluorescence anisotropy decay in picosecond time region, which was measured with the TCPC system. The anisotropy decay shows a rather slow decay which is fitted well with a single-exponential decay with a time constant of 30 ps. The anisotropy decay in femtosecond time region is shown in Figure 5b, which was obtained with fluorescence upconversion technique. It is seen that an oscil-

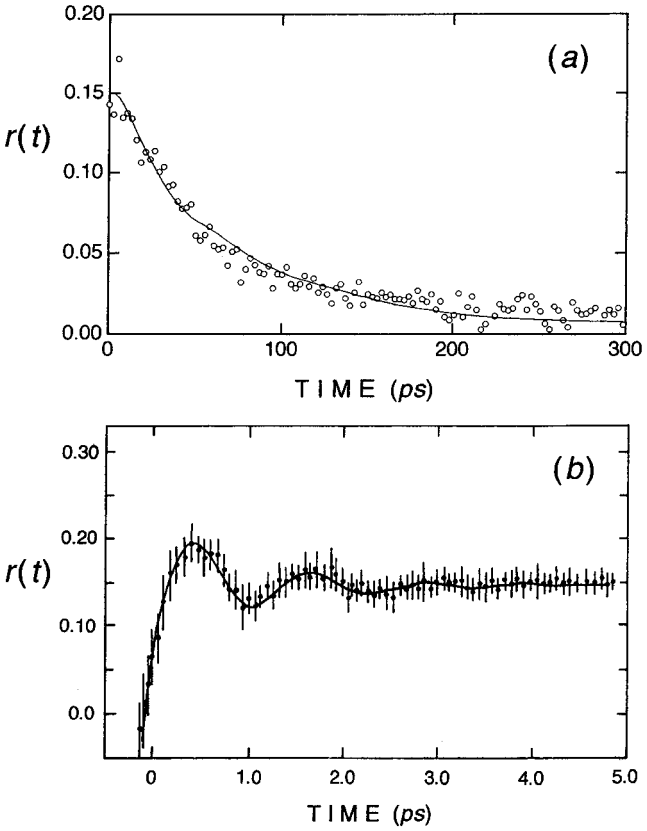

Figure 5. (a) Picosecond fluorescence anisotropy decay measured with the TCPC apparatus. The excitation wavelength is 408 nm, and the monitoring wavelength is 450 nm. (b) Femtosecond fluorescence anisotropy decay of DTA in THF, measured with the fluorescence up-conversion apparatus. The excitation and monitoring wavelengths are the same as those in (a). The standard deviation in four sets of measurements is shown in vertical lines.

lating pattern is superimposed to the anisotropy decay in 0−4 ps, and that the anisotropy starts from a certain negative value as is seen around $t = 0$. A detailed analysis of the oscillatory pattern will be presented in the Discussion section.

4. Discussion

4.1. Theory of the Recurrence Motion of an Excitation. The recurrence of the excitation energy transfer in a molecular system consisting of two identical chromophores can be described in principle by the degenerate-state perturbation theory. Note that, in the present case of DTA, the orientations of two anthracene rings are not exactly orthogonal; the angle between the two short axes is 88.5° from the X-ray crystallography. The 0.5° displacement from the orthogonal orientation creates a dipole−dipole interaction. Furthermore, as will be discussed later, the magnitude of the interaction energy depends also on the angle between the electronic transition dipole moment for $S_1(^1L_a)$—S_0 and the short molecular axis in one anthracene moiety. Figure 6 illustrates a scheme of interchromophore interaction related to the resonance energy transfer between two identical chromophores. A singly excited state of this system is described as a product of the wave functions of the excited state of moiety ***a***, $ø_a'$, and the ground state of another moiety ***b***, $ø_b$, i.e., $\phi_1 = ø_a' ø_b$ (the prime stands for the excited state). Similarly the other excited state of the system is defined as $\phi_2 = ø_a ø_b'$. These two degenerate states ϕ_1 and ϕ_2, which are the eigenfunctions of the zeroth-order Hamiltonian H_0, can interact each other through a Coulombic resonance interaction

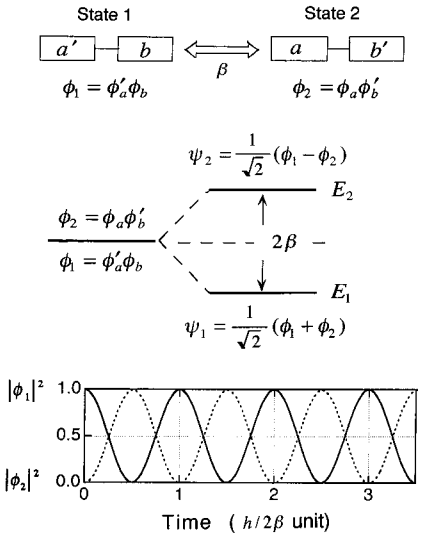

Figure 6. Diagramatic illustration of the dipole−dipole interaction (β) between the two degenerate states ϕ_1 and ϕ_2 and the creation of the two superposition states ψ_1 and ψ_2 split by 2β. When the two states are excited coherently with an ultrashort pulse laser, the quantum state undergoes a time evolution. The recurrence motion of excitation is shown in the bottom.

which can be approximated as a dipole−dipole interaction. From the first-order perturbation calculation, the resonance interaction creates two superposition states $\psi_1 = (1/\sqrt{2})(\phi_1 + \phi_2)$ and $\psi_2 = (1/\sqrt{2})(\phi_1 - \phi_2)$ which are the time-independent states appearing in the static spectrum with a splitting of the interaction energy 2β. When the two superposition states are excited coherently by an ultrashort light pulse, the quantum state is no longer a stationary state and undergoes a time evolution expressed as

$$\Psi(t) = \frac{1}{\sqrt{2}}\psi_1 e^{-iE_1 t/\hbar} + \frac{1}{\sqrt{2}}\psi_2 e^{-iE_2 t/\hbar} \qquad (1)$$

for the particular case when molecule ***a*** is initially excited. Taking the probability density of the quantum state in eq 1, we obtain

$$|\Psi(t)|^2 = (1/2)\psi_1^{\,2} + (1/2)\psi_2^{\,2} + \psi_1\psi_2 \cos[(E_1 - E_2)t/\hbar] \qquad (2)$$

where the third term manifests a time evolution generated from an interference between ψ_1 and ψ_2. Rewriting eq 2 by using the original basis functions ϕ_1 and ϕ_2, we obtain the following equation:

$$|\Psi(t)|^2 = \cos^2(\beta t/\hbar)\,\phi_1^{\,2} + \sin^2(\beta t/\hbar)\,\phi_2^{\,2} \qquad (3)$$

This alternative equation provides us with a more appropriate expression that an excitation localized on either half of a bichromophore moves back and forth between two chromophores with a time period of $h/2\beta$. The recurrence motion of excitation is illustrated in Figure 6. One should note here that the theoretical scheme mentioned above is for a special case in which one molecule is initially excited, and that actually there is a continuum of different initial conditions making different superpositions that are used in an average over the ensemble. Also noteworthy is that such a recurrence could appear, however, only in a short time (<1 ps) because the electronic dephasing process will be so fast that the macroscopic quantum coherence is lost rapidly in the condensed phase.

Usually, molecules in solution undergo solute−solvent interactions which will change at each instant the electronic transition frequency and the energy transfer interaction. Such random and chaotic modification of the energy transfer interaction causes the reaction dynamics of an ensemble to change from a coherent to an incoherent process. To analyze the coherent reaction dynamics involving the dephasing process, the quantum mechanical treatment is performed on the basis of the density matrix. We here analyze the experimental results following a theoretical formulation derived by Kim et al.,[5] Zhu et al.,[6] and Wynne and Hochstrasser.[8−10] The time evolution of the density matrix elements ρ_{11} and ρ_{22}, i.e., populations of states ϕ_1 and ϕ_2, respectively, can be expressed by the following differential equation which is derived from the optical Bloch equations:[12]

$$\Delta\ddot{n} + \left(\frac{1}{T_1} + \frac{2}{T_2}\right)\Delta\dot{n} + \left(4\beta^2 + \frac{2}{T_1T_2}\right)\Delta n = 0 \qquad (4)$$

where Δn is the population difference $\Delta n = \rho_{11} - \rho_{22}$; β is the resonance transfer interaction energy; and the phenomenological decay times T_1 for populations and T_2 for coherence are connected in a relation $1/T_2 = 1/(2T_1) + 1/T_2'$, where T_2' is the pure dephasing time (i.e., the decay of ρ_{12}). The differential equation of eq 4 can be solved for the cases depending on the relative magnitudes of the interaction energy 2β and the energy width of the dephasing process (T_2'). In the underdamped condition $2\beta\ T_2' > 1$, the solution is obtained as follows:[9]

$$\Delta n(t) = \Delta n(0)e^{-(1/T_1+1/T'_2)t}\left[\frac{1}{T'_2\omega}\sin(\omega t) + \cos(\omega t)\right]$$
$$= \Delta n(0)e^{-(1/T_1+1/T'_2)t}\cos(\omega t + \delta) \qquad (5)$$

where $\omega = \sqrt{4\beta^2 - (1/T_2')^2}$ and $\sin\delta = -1/\omega\ (1/T_1 + 1/T_2')$. A sum of populations $S = \rho_{11} + \rho_{22}$ is derived also from Bloch equations as follows:

$$S(t) = e^{-(1/T_1)t}S(0) \qquad (6)$$

Equation 5 shows that the population difference $\rho_{11} - \rho_{22}$ oscillates at an angular frequency ω, but the oscillation does not continue indefinitely and is damped with a rate $1/T_1 + 1/T_2'$. Equation 6 shows that the sum of populations $\rho_{11} + \rho_{22}$ decays exponentially with a rate $1/T_1$.

In an experiment to observe such a recurrence motion of excitation by probing the polarized fluorescence, we need to correlate the propagators for the density matrix elements ρ_{11}, ρ_{12}, ρ_{21} and ρ_{22} with the polarized fluorescence intensity. The magnitude of the density matrix element depends not only on the strength of the transition dipole moment, but also on the projection of the pump pulse polarization in the laboratory frame onto the transition dipole moment vector. The polarized fluorescence intensities are obtained after calculation of the stochastic averages of the correlation functions for an isotropic medium as follows:[8,10]

$$I(t) = 2\langle l_x l_y p_x p_y\rangle e^{-\gamma t} + \langle l_x^2 p_x^2\rangle[1 + f(t)] + \langle l_x^2 p_y^2\rangle[1 - f(t)] \qquad (7)$$

where $f(t)$ is the term of the damped oscillation in eq 5, i.e.,

$$f(t) = e^{-(1/T_1+1/T_2')t}\cos(\omega t + \delta) \qquad (8)$$

l_i, m_i, and n_i *are* the direction cosines of the field polarization vector onto the molecular polarization dipole i; and p_i is that for the probe emission polarization. We consider first the case where the electronic transition dipole moments coincide between the excitation absorption and the probe fluorescence as shown in Figure 7 a. If p_i is chosen parallel to the pump polarization, we obtain $I_{||}(t)$ with the substitutions $p_x = l_x$, $p_y = l_y$, and if it is perpendicular we obtain $I_\perp(t)$ with the substitutions $p_x = m_x$, $p_y = m_y$. After calculating the average of the correlation function, the anisotropy is expressed as[8−10]

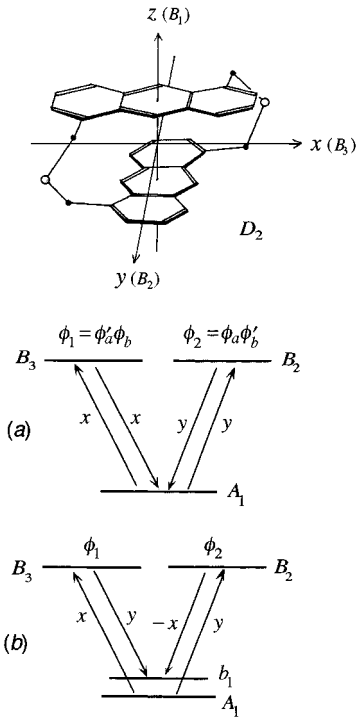

Figure 7. Energy level scheme with symmetries of states and directions and signs of transition dipole moments in the frame of a molecule with D_2 symmetry. The *x*- and *y*-axes are taken to be orthogonal to the D_2 rotation axis (*z*-axis). (a) The usual case for fluorescence. (b) An alternative case that involves out-of-plane (*z*-polarized) transition due to involvement of a b_1 vibrational state in the final electronic state.

$$r(t) = \frac{I_{11}(t) - I_\perp(t)}{I_{11}(t) + 2I_\perp(t)} = \frac{1}{10}[1 + 3f(t) + 3e^{-\gamma t}] \qquad (9)$$

where $\gamma = 2/T_2'$. It is worth noting that $I_{||}(t) + 2I_\perp(t)$ is a constant value 10/15, suggesting that the isotropic decay shows no oscillation. In the case of a dimer as in the present case of DTA, the equation for $r(t)$ is expressed as[13]

$$r_D(t) = \frac{r(t) + \frac{1}{10}[3 + e^{-\gamma t} - 3f(t)]\cos^2\theta}{1 + e^{-\gamma t}\cos^2\theta} \qquad (10)$$

where θ is the angle between the transition dipole moments of two chromophores. Since θ is near 90° and $\cos\theta \approx 0$ in DTA, eq 9 is the proper one to be used for analyzing the present experiments. Therefore, an analysis of the oscillatory pattern based on eq 9 provides us with information on the interchromophore interaction energy and the electronic dephasing time.

4.2. Fluorescence Decay and Anisotropy Decay in the Picosecond Region. The decay constants obtained from the fluorescence decay and anisotropy decay in the picosecond time regime are summarized in Table 1. In our previous study,[7] it was found that the 63-ps fluorescence lifetime corresponds to the time constant of relaxation from locally excited anthracene

TABLE 2: Comparison of Characteristics of the Coherent Energy Transfer Dynamics of DTA and Binaphthyl in Solution

molecules	dephasing time T_2' (ps)	oscillation period (ps)	interaction energy 2β (cm^{-1})	$2\beta\ T_2'$	rotational diffusion τ_R (ps)
DTA[a] (THF)	1.0	1.2	28.6	2.73	30.0
binaphthyl[b](CCl_4)	0.18	1.2	41	1.4	34.5
binaphthyl[b] (*n*-hexane)	0.14	2.9	40	1.1	24.6

[a] Present work. [b] Ref 6.

to an excimer and the 3.2-ns lifetime to the excimer deactivation. Although the excimer fluorescence is involved in the emission signal monitored at 450 nm, we can safely ignore the 3.2-ns decay component for the present analysis. Then it follows that the population decay time for $\rho_{11} + \rho_{22}$ is $T_1 = 63 \pm 1$ ps. The 30-ps time constant in the picosecond anisotropy decay can be regarded as due to that of the rotational diffusion of DTA in THF solution. Since this overall reorientational motion of DTA in THF solution occurs on a much slower time scale than the energy transfer, the internal angular jump of excitation could be viewed as occurring in a relatively fixed dimer orientation.

4.3. Analysis of Fluorescence Anisotropy. The theoretical equation for the fluorescence anisotropy decay is given in eq 9 for a pair of chromophores coupled by an energy transfer interaction.[8−10] This equation holds for the usual case where the electronic transition dipole moments coincide between the excitation absorption and the probe fluorescence, as shown in Figure 7a. Equation 9 predicts that the anisotropy at very short time before dephasing has a value of $r = 0.7$, then this value decreases to $r = 0.4$ due to electronic dephasing. When the two degenerate states ϕ_1 and ϕ_2 are completely dephased by the incoherent coupling, the anisotropy attains a value of $r = 0.1$. Contrary to the theoretical prediction for the usual case, however, the experimental anisotropy decay $r(t)$ shown in Figure 5a commences with a negative value at $t = 0$ and then it converges on $r(t) = +0.15$ after damping oscillation. We assume, therefore, that another fluorescence component with its anisotropy being a negative value at $t = 0$ is involved in the probed fluorescence. In the case that the final state of fluorescence transition is a vibrational state of a nontotally symmetric vibration, the fluorescence transition moment could be perpendicular to the absorption transition moment. This view might be supported by the experimental condition that the anisotropy decay is monitored at 450 nm, i.e., a spectral region corresponding to a vibrational level of 1800 cm^{-1} above the 0−0 transition energy.

For the case that the fluorescence transition dipole is perpendicular to the absorption dipole through a coupling to a nontotally symmetric vibration in the final state, as shown in Figure 7b, the expression for $I_{||}(t)$ is obtained from eq 7 with the substitutions $p_x = l_y$, $p_y = -l_x$ as $(2/15)\{2 - f(t) - e^{-\gamma t}\}$, and that for $I_\perp(t)$ is obtained with the substitutions $p_x = m_y$, $p_y = -m_x$ as $(1/15)\{3 + f(t) + e^{-\gamma t}\}$. As a result, we obtain the anisotropy decay as

$$r(t) = \frac{1}{10}\{1 - 3f(t) - 3e^{-\gamma t}\} \qquad (11)$$

One should note that $I_{||}(t) + 2I_\perp(t)$ is a constant value 10/15 as in the usual case mentioned before. Equation 11 shows that the value of anisotropy is $r = -0.5$ at $t = 0$, then $r = -0.2$ after dephasing and $r = 0.1$ after population equalization. We assume that the fluorescence monitored at 450 nm is a superposition of two vibronic transitions; the one is coupled to a totally symmetric vibration and the other coupled to a nontotally b_1 vibration. The resultant time-dependent anisotropy is a sum of the two anisotropy curves of eqs 7 and 11. The best fit curve was obtained with the ratio 1:0.35 of the amplitude of the former function in eq 9 to that of the latter function in eq 11. The solid line in Figure 5b is the best fit to the experimental curve. We obtain $\omega = (5.2 \pm 0.2) \times 10^{12}$ rad s^{-1} and $T_2' = 1.0 \pm 0.1$ ps leading to the resonance energy transfer interaction $2\beta = 28.6$ cm^{-1}.

Note that DTA has D_2 symmetry and the states ϕ_1 and ϕ_2 belong to B_2 and B_3 symmetry classes, respectively. The vibrational state which gives the transition dipoles perpendicular to the absorption transition should have b_1 symmetry. From the MO calculation using the PM3 method as parametrized within the MOPAC 93.0,[14] DTA has several normal vibrations belonging b_1 symmetry in a range of ~1800 cm^{-1}. Therefore, the probed fluorescence is due to the transition from a level of ^1L_a (0−0) to a vibronic level of one vibrational quantum of b_1 symmetry mode.

4.4. Magnitude of the Dipole−Dipole Interaction between Chromophores in DTA. The dipole−dipole interaction energy is expressed as

$$\beta = \frac{1}{4\pi\epsilon_0\epsilon}\frac{e^2|\mathbf{M}|^2}{R^3}(\cos\theta_{12} - 3\cos\theta_{1R}\cos\theta_{2R}) \qquad (12)$$

where e is the elementary charge, $\mathbf{M}$ is the transition dipole moment, R is the distance between the centers of chromophores, ϵ_0 and ϵ are the permittivities of free space and of the solvent (THF), respectively, θ_{12} is the angle between the transition dipoles of two chromophores, θ_{1R} is the angle between the transition moment of the one chromophore and the distance vector, and θ_{2R} is for the other chromophore. Values of these parameters except for θ_{12} are available from the experimental data and literature, i.e., $\mathbf{M} = 0.578 \times 10^{-10}$ m (estimated from the oscillator strength $f = 0.1$[15]), $R = 3.41$ Å ,and $\epsilon = 7.58$ (THF). For the orientational factor, $\cos\theta_{1R} = \cos\theta_{2R} = 0$, while θ_{12} is unknown although the angle between the two anthracene rings is known to be 0.5°. From the MO calculation with the CNDO/S3 by MOPAC 93.0[14] for anthracene-1,5-dimethanethiol, the angle between the transition moment and the short axis of the anthracene ring is estimated to be 4.5°, and therefore θ_{12} is 81.0°. By using these parameter values the interaction energy is estimated to be $2\beta = 40.4$ cm^{-1}. This value is in an acceptable agreement with the value obtained from the analysis of oscillatory anisotropy decay ($2\beta = 29$ cm^{-1}).

4.5. Comparison of the Two cases; DTA and Binaphthyl. Hochstrasser and co-workers[6] reported the coherent excitation transfer in 2,2′-binaphthyl in different solvents at room temperature. The transient absorption anisotropy decay in CCl_4 exhibited a damped oscillation with a time period of 1.2 ps and a damping time constant of 180 fs. They found from the theoretical analysis that the anisotropy oscillation arises from the energy transfer recurrence among two naphthyl moieties associated with $2\beta = 41$ cm^{-1} and $T_2' = 0.2$ ps. Table 2 summarizes the numerical parameters for the two cases of DTA and binaphthyl. Comparing the case of binaphthyl with the case of DTA, one can see that the dephasing time is longer in DTA by a factor of 5 than in binaphthyl, while the interaction energy

is smaller in DTA than in binaphthyl. Significantly longer dephasing time of DTA can be interpreted as due to a rigid dimer conformation of DTA leading to a fixed relative orientation of the two anthracene rings. The dimeric structure of binaphthyl in turn is flexible with respect to relative orientation of the two chromophores by twisting around the single bond, and is subject to fluctuating forces which may reduce the electronic dephasing time. Consequently, the key parameter for the coherent dynamics $2\beta T_2'$ is 2.73 in DTA significantly larger than in binaphthyl (1.1−1.4). This means that in DTA the longer dephasing time predominantly is responsible for the appearance of excitation recurrence. If the dephasing time of DTA is comparable to that of binaphthyl, $2\beta T_2'$ is less than unity (the overdamped case), and there appear neither oscillatory behavior nor coherent dynamics.

5. Concluding Remarks

We have observed a damped oscillation superimposed onto the fluorescence anisotropy decay in DTA in THF at room temperature. The oscillatory behavior was analyzed using the theoretical formula developed by Wynne and Hochstrasser[8−10] for the recurrence motion of an excitation among coupled chromophores. From the apparent oscillation period of 1.2 ps and the dephasing time of 1.0 ps, the interaction energy was estimated to be $2\beta = 28.6$ cm^{-1} which is in acceptable agreement with the theoretical value of the dipole−dipole resonance interaction between two anthracene rings in DTA (40 cm^{-1}). The damping time constant is 1.0 ps significantly longer than in the case of binaphthyl. A fairly slow dephasing time can be regarded as due to a rigid structure of the dimeric conformation of DTA. An interpretation remains tentative, however, for the anisotropy decay which starts from a negative value, contrary to the usual case where the transition dipole moments for absorption and fluorescence are identical and $r(0) = +0.7$. This disagreement has been explained in this paper as an additional contribution from another fluorescent component due to a vibronic transition with a nontotally symmetric vibration. Although such a contribution and its anisotopy behavior are predicted theoretically,[4,8] further study on vibrational modes in DTA will be needed to get a fully consistent picture for this problem.

The present study provides an additional example of the coherent energy transfer dynamics in organized molecular systems. Particularly the present study demonstrates that a rigid and fixed conformation between the reacting chromophores play an important role in reducing the electronic dephasing rate, and leading the molecular system into the underdamped condition $2\beta T_2' > 1$. Further experimental studies on the coherent energy transfer will be presented in a forthcoming paper for another type of dimeric structure of anthracene chromophores. As a future work along this line, it would be interesting to investigate the effect of breaking the site-energy degeneracy of the chromophores by adding various substituent groups to one of them.

Acknowledgment. The present work is supported by a Grant-in-Aid for Scientific Research on Priority Areas (B) (No. 11223203) from the Ministry of Education, Science, Sports, and Culture of Japan. The authors acknowledge the reviewers of the present paper for their fruitful discussion and comments.

References and Notes

(1) Förster, T. In *Modern Quantum Chemistry*; Sinanoglu, O., Ed.; Academic Press: New York, 1965; Part III, p 93.

(2) Rahman, T. S.; Knox, R. S.; Kenkre, V. M. *Chem. Phys.* **1979**, *44*, 197.

(3) Knox, R. S.; Gülen, D. *Photochem. Photobiol.* **1993**, *57*, 40.

(4) Matro, A.; Cina, J. A. *J. Phys. Chem.* **1995**, *99*, 2568.

(5) Kim, Y. P.; Share, P.; Pereira, M.; Sarisky, M.; Hochstrasser, R. M. *J. Chem. Phys.* **1989**, *91*, 7557.

(6) Zhu, F.; Galli, C.; Hochstrasser, R. M. *J. Chem. Phys.* **1993**, *98*, 1042.

(7) Sakata, Y.; Toyoda, T.; Yamazaki, T.; Yamazaki, I. *Tetrahedron Lett.* **1992**, *33*, 5077.

(8) Wynne, K.; Hochstrasser, R. M. *Chem. Phys.* **1993**, *171*, 179.

(9) Wynne, K.; Gnanakaran, S.; Galli, C.; Zhu, F.; Hochstrasser, R. M. *J. Lumin.* **1994**, *60/61*, 735.

(10) Wynne, K.; Hochstrasser, R. M. *J. Raman Spectrosc.* **1995**, *26*, 561.

(11) Kuritani, M.; Sakata, Y.; Ogura, F.; Nakagawa, M. *Bull. Chem. Soc. Jpn.* **1973**, *46*, 605.

(12) Allen, L.; Eberly, J. H. *Optical Resonance and Two-level Atoms*; Wiley- Interscience: New York, 1975.

(13) The correct expression for $r_D(t)$ is given in ref 9. One can derive this equation with reference to ref 8 and the paper, van Amerongen, H.; Struve, W. S. *Methods Enzymol.* **1995**, *246*, 259.

(14) (a) Dewar, M. J. S.; Zoebisch, E. G.; Healy, E. F.; Stewart, J. J. P. *J. Am. Chem. Soc.* **1985**, *107*, 3902. (b) Stewart, J. J. P. MOPAC 93.0 Manual; Fujitsu Limited: Tokyo, 1993.

(15) Murrell, J. N.; Tanaka, J. *Mol. Phys.* **1964**, *7*, 363.